

## Crystal Structures of Oxidized and Reduced Stellacyanin from Horseradish Roots<sup>†</sup>

Michael Koch,<sup>‡</sup> Milko Velarde,<sup>‡</sup> Mark D. Harrison,<sup>§</sup> Steffi Echt,<sup>||</sup> Markus Fischer,<sup>||</sup>  
Albrecht Messerschmidt,<sup>\*‡</sup> and Christopher Dennison<sup>\*§,⊥</sup>

*Contribution from the Abteilung Strukturforschung, Max-Planck-Institut für Biochemie, Am Klopferspitz 18, D-82152 Martinsried, Germany, School of Natural Sciences, Bedson Building, University of Newcastle upon Tyne, Newcastle upon Tyne, NE1 7RU, U.K., and Lehrstuhl für Organische Chemie und Biochemie, Technische Universität München, Lichtenbergstrasse 4, D-85747 Garching, Germany*

Received June 28, 2004; E-mail: messersc@biochem.mpg.de; christopher.dennison@ncl.ac.uk

**Abstract:** Umecyanin (UMC) is a type 1 copper-containing protein which originates from horseradish roots and belongs to the stellacyanin subclass of the phytoeyanins, a ubiquitous family of plant cupredoxins. The crystal structures of Cu(II) and Cu(I) UMC have been determined at 1.9 and 1.8 Å, respectively. The protein has an overall fold similar to those of other phytoeyanins. At the active site the cupric ion is coordinated by the N<sup>δ1</sup> atoms of His44 and His90, the S<sup>γ</sup> of Cys85, and the O<sup>ε1</sup> of Gln95 in a distorted tetrahedral geometry. Both His ligands are solvent exposed and are surrounded by nonpolar and polar side chains on the protein surface. Thus, UMC does not possess a distinct hydrophobic patch close to the active site in contrast to almost all other cupredoxins. UMC has a large surface acidic patch situated ~10–30 Å from the active site. The structure of Cu(I) UMC is the first determined for a reduced phytoeyanin and demonstrates that the coordination environment of the cuprous ion is more trigonal pyramidal. This subtle change in geometry is primarily due to the Cu–N<sup>δ1</sup>(His44) and Cu–O<sup>ε1</sup>(Gln95) bond lengths increasing from 2.0 and 2.3 Å in Cu(II) UMC to 2.2 and 2.5 Å, respectively, in the reduced form, as a consequence of slight rotations of the His44 and Gln95 side chains. The limited structural changes upon redox interconversion at the active site of this stellacyanin are analogous to those observed in a typical type 1 copper site with an axial Met ligand and along with its surface features suggest a role for UMC in interprotein electron transfer.

### Introduction

Cupredoxins are a key class of electron-transfer (ET) proteins found in both prokaryotes and eukaryotes which possess a mononuclear type 1 copper site.<sup>1</sup> Stellacyanins are members of the phytoeyanin subclass of the cupredoxins which are found in all vascular seed plants and whose exact physiological function remains unknown.<sup>1–3</sup> The phytoeyanin family also includes the plantacyanins and the uclacyanins, and their division has been made on the basis of domain organization, glycosylation, and the nature of the axial ligand.<sup>2</sup> Sequence comparisons have indicated that all stellacyanins possess an axially coordinating glutamine whereas the plantacyanins and uclacyanins, and most other cupredoxins, have a Met ligand.<sup>1–3</sup> The

stellacyanins are all thought to possess associated carbohydrate and a cell wall anchoring domain.<sup>2</sup> Umecyanin (UMC) is the stellacyanin from *Armoracia laphatifolia* (horseradish) roots,<sup>4</sup> and paramagnetic NMR studies on the Ni(II)-substituted protein have recently confirmed the presence of an axially coordinating glutamine.<sup>5</sup>

Crystallographic studies on a number of cupredoxins have demonstrated that their overall structures are alike,<sup>6–12</sup> consisting of  $\beta$ -strands arranged into two  $\beta$ -sheets forming a Greek key  $\beta$ -barrel structure (the so-called “cupredoxin” fold). There are variable amounts of  $\alpha$ -helical secondary structure present, but this never contributes to the core of the protein. The copper ion is situated at one extreme of the molecule and is usually coordinated in a distorted tetrahedral fashion, with strong ligands

<sup>†</sup> The atomic coordinates of Cu(II) (1X9R) and Cu(I) (1X9U) UMC have been deposited in the Protein Data Bank.

<sup>‡</sup> Max-Planck-Institut für Biochemie.

<sup>§</sup> University of Newcastle upon Tyne.

<sup>||</sup> Technische Universität München.

<sup>⊥</sup> Present address: Institute for Cell and Molecular Biosciences, University of Newcastle upon Tyne.

(1) Nersissian, A. M.; Shipp, E. L. *Adv. Protein Chem.* **2002**, *60*, 271–340.  
(2) Nersissian, A. M.; Immoos, C.; Hill, M. G.; Hart, P. J.; Williams, G.; Herrmann, R. G.; Valentine, J. S. *Protein Sci.* **1998**, *7*, 1915–1929.  
(3) Dennison, C.; Harrison, M. D.; Lawler, A. T. *Biochem. J.* **2003**, *371*, 377–383.

(4) Paul, K. G.; Stigbrand, T. *Biochim. Biophys. Acta* **1970**, *221*, 255–263.  
(5) Dennison, C.; Harrison, M. D. *J. Am. Chem. Soc.* **2004**, *126*, 2481–2489.  
(6) Adman, E. T. *Adv. Protein Chem.* **1991**, *42*, 144–197.  
(7) Adman, E. T. *Curr. Opin. Struct. Biol.* **1991**, *1*, 895–904.  
(8) Colman, P. M.; Freeman, H. C.; Guss, J. M.; Murata, M.; Norris, V. A.; Ramshaw, J. A. M.; Venkatappa, M. P. *Nature* **1978**, *272*, 319–324.  
(9) Inoue, T.; Nishio, N.; Suzuki, S.; Kataoka, K.; Kohzuma, T.; Kai, Y. *J. Biol. Chem.* **1999**, *274*, 17845–17852.  
(10) Adman, E. T.; Jensen, L. H. *Isr. J. Chem.* **1981**, *21*, 8–12.  
(11) Nar, H.; Messerschmidt, A.; Huber, R.; van de Kamp, M.; Canters, G. W. *J. Mol. Biol.* **1991**, *221*, 765–772.  
(12) Crane, B. R.; Di Bilio, A. J.; Winkler, J. R.; Gray, H. B. *J. Am. Chem. Soc.* **2001**, *123*, 11623–11631.

provided by the thiolate sulfur of a Cys and the imidazole nitrogens of two His residues. The active site structure is typically completed by an unusually long bond to an axial Met ligand. In the case of azurin the backbone carbonyl oxygen of a Gly residue provides a second axial ligand, resulting in a trigonal bipyramidal geometry.<sup>10–12</sup> The His<sub>2</sub>Cys equatorial ligand set is always maintained in cupredoxins, but the residue found in the axial position can vary, as in the stellacyanins, where a Gln coordinates.<sup>5,13,14</sup> The imidazole group of the C-terminal His ligand is always solvent exposed and is surrounded by a surface hydrophobic patch which is important for the interaction of cupredoxins with their redox partners.<sup>15–17</sup>

The crystal structures of three phytoeyanins have been solved in the oxidized forms. These are the stellacyanin from *Cucumis sativus* (CST<sup>13</sup>) and the plantacyanins from *C. sativus* (this protein is commonly referred to as cucumber basic protein, CBP<sup>18</sup>) and spinach (PNC<sup>19</sup>). The structures of these proteins have a number of unusual features as compared to other cupredoxins including a disulfide bridge which connects an active site loop with an  $\alpha$ -helix, and a twist in one of the  $\beta$ -sheets that makes up the  $\beta$ -barrel, giving a topology which has been described as a  $\beta$ -sandwich.<sup>18</sup> The nature of the phytoeyanin fold is such that the imidazole rings of both His ligands are solvent exposed. The unusual active site geometry of the stellacyanins was demonstrated by the structure of the *C. sativus* protein, where the axial Gln ligand was found to coordinate in a monodentate fashion via its side chain amide oxygen atom,<sup>13</sup> which is supported by paramagnetic <sup>1</sup>H NMR studies.<sup>5</sup>

It has been noted<sup>1</sup> that the phytoeyanins may represent one of the largest families of plant proteins (at least 50 sequences are expected to be found in the *Arabidopsis thaliana* genome). This observation and the fact that the exact physiological function of phytoeyanins remains unknown make them a key target for investigation. Furthermore, the influence of the natural type 1 copper site variation found in the stellacyanins on ET reactivity is not well understood. In this paper, we present the crystal structure of both oxidized and reduced UMC. The structure of Cu(I) UMC is the first determined for a reduced phytoeyanin and along with the surface properties of the molecule provides information which is key to understanding the physiological function of these ubiquitous plant proteins.

## Material and Methods

**Protein Isolation and Purification.** *Escherichia coli* BL21(DE3) cells were transformed with a pET11a derivative harboring an artificial coding region for the 106 amino acid residue cupredoxin domain of UMC (Glu1 to Gly106) which was synthesized in a manner described elsewhere.<sup>20</sup> This construct also contains an N-terminal start codon (Met0) as a translation initiator which is present in the purified protein.<sup>20</sup>

Overexpression, refolding, and purification of UMC were as described elsewhere,<sup>20</sup> and the protein was used at a concentration of ca. 11 mg/mL in 5 mM Tris (pH 7.5) for crystallization experiments.

**Crystallization and Crystal Preparation.** Crystallization of oxidized UMC was achieved with a reservoir buffer containing 25% PEG 3350, 0.1 M Bicine (pH 5.0), and 0.2 M MgCl<sub>2</sub>. Crystals were grown using the sitting drop method by adding 2  $\mu$ L of the reservoir buffer to 2  $\mu$ L of the protein solution. Crystals with a maximum size of 400  $\times$  300  $\times$  300  $\mu$ m were obtained which could be frozen by soaking in a cryobuffer (made by adding 10% PEG 600 to the reservoir buffer). A crystal of Cu(II) UMC was reduced using cryobuffer containing 10 mM sodium ascorbate. Reduction was considered to be complete when the crystal was totally colorless.

**Data Collection.** Data sets were collected on a Mar345 imaging plate detector system (Marresearch, Nordstedt, Germany) with graphite-monochromated Cu K $\alpha$  radiation ( $\lambda = 1.5418$  Å) at 50 kV/100 mA from a Rigaku (Tokyo, Japan) RU 300 rotating anode X-ray generator at 100 K to a resolution of 1.9 Å for Cu(II) UMC and 1.8 Å for the reduced protein. Photoreduction of Cu(II) UMC did not occur as judged from the color of the crystal before and after data collection. The crystal of Cu(I) UMC was still completely colorless after the data set was collected, indicating no oxidation had occurred. Determination of the space group and unit cell, as well as the integration of reflection intensity, was carried out with the program DENZO.<sup>21</sup> Further data analysis was performed with the HKL program package.<sup>21</sup> The data collection and refinement statistics are shown in Table 1.

**Structure Solution and Refinement.** The initial phases of the oxidized UMC structure were determined by molecular replacement with the program AMoRe<sup>22</sup> using the *C. sativus* stellacyanin structure (PDB entry 1JER<sup>13</sup>) as the template. After initial rigid body minimization,<sup>23</sup> refinement was performed by alternating model building carried out with the program O<sup>24</sup> and crystallographic refinement using CNS.<sup>23,25</sup> All graphical representations were prepared using the programs MOLSCRIPT,<sup>26</sup> BOBSCRIPT,<sup>27</sup> RASTER3D,<sup>28</sup> ALSRIPT,<sup>29</sup> and GRASP.<sup>30</sup> Final Ramachandran plot analysis was performed with the program PROCHECK.<sup>31</sup> For the superposition of the different 3D structures, the program LSQMAN<sup>32</sup> was applied.

## Results

**Quality of the Final Model.** The refined models for the oxidized and reduced forms of UMC each comprise one homodimer, two copper ions, and 272 or 215 water molecules, respectively, and maintain small deviations from standard geometry (Table 1). In both structures, the residues Met0, Gly105, and Gly106 are missing in both subunits of the dimer and Ala104 in molecule B only because there was no electron density observed for these residues. The final crystallographic *R*-factor and free *R*-factor are 21.8% and 26.5% (1.9 Å resolution) for the oxidized form and 19.9% and 24.4% for the reduced one (1.8 Å resolution). The mean positional errors of

- (13) Hart, P. J.; Nersissian, A. M.; Herrmann, R. G.; Nalbandyan, R. M.; Valentine, J. S.; Eisenberg, D. *Protein Sci.* **1996**, *5*, 2175–2183.
- (14) Vila, A. J.; Fernández, C. O. *J. Am. Chem. Soc.* **1996**, *118*, 7291–7298.
- (15) Chen, L.; Durlay, R.; Poliks, B. J.; Hamada, K.; Chen, Z.; Mathews, F. S.; Davidson, V. L.; Satow, Y.; Huizinga, E.; Vellieux, F. M. D.; Hol, W. G. *J. Biochemistry* **1992**, *31*, 4959–4964.
- (16) Ubbink, M.; Ejdeback, M.; Karlsson, B. G.; Bendall, D. S. *Structure* **1998**, *6*, 323–335.
- (17) Crowley, P. B.; Otting, G.; Schlarb-Ridley, B. G.; Canters, G. W.; Ubbink, M. *J. Am. Chem. Soc.* **2001**, *123*, 10444–10453.
- (18) Guss, J. M.; Merritt, E. A.; Phizackerley, R. P.; Freeman, H. C. *J. Mol. Biol.* **1996**, *262*, 686–705.
- (19) Einsle, O.; Mehrabian, Z.; Nalbandyan, R.; Messerschmidt, A. *J. Biol. Inorg. Chem.* **2000**, *5*, 666–672.
- (20) Harrison, M. D.; Dennison, C. *Proteins* **2004**, *55*, 426–435.

- (21) Otwinowski, Z.; Minor, W. *Methods Enzymol.* **1997**, *276*, 307–326.
- (22) Navaza, J. *Acta Crystallogr.* **1994**, *A50*, 157–163.
- (23) Brunger, A. T.; Adams, P. D.; Clore, G. M.; DeLano, W. L.; Gros, P.; Grosse-Kunstleve, R. W.; Jiang, J. S.; Kuszewski, J.; Nilges, M.; Pannu, N. S.; Read, R. J.; Rice, L. M.; Simonson, T.; Warren, G. L. *Acta Crystallogr.* **1998**, *D54*, 905–921.
- (24) Jones, T. A.; Zou, J. Y.; Cowan, S. W.; Kjeldgaard, M. *Acta Crystallogr.* **1991**, *A47*, 110–119.
- (25) Brunger, A. T. *Nature* **1992**, *355*, 472–475.
- (26) Kraulis, P. J. *J. Appl. Crystallogr.* **1991**, *24*, 946–950.
- (27) Esnouf, R. M. *J. Mol. Graphics Modell.* **1997**, *15*, 132–134.
- (28) Merritt, E. A.; Bacon, D. J. *Methods Enzymol.* **1997**, *277*, 505–524.
- (29) Barton, G. J. *Protein Eng.* **1993**, *6*, 37–40.
- (30) Nichols, A.; Sharp, K.; Honig, B. *Proteins* **1991**, *11*, 281–296.
- (31) Laskowski, R. A.; MacArthur, M. W.; Moss, D. S.; Thornton, J. M. *J. Appl. Crystallogr.* **1993**, *26*, 283–291.
- (32) Kleywegt, G. J.; Jones, T. A. *A Super Position*; ESF/CCP4 Newsletter; 1994; Vol. 31, pp 9–14.

**Table 1.** Data Collection and Refinement Statistics

data set	Cu(II) UMC	Cu(I) UMC
	Data Collection	
no. of unique reflns	18450	21408
multiplicity <sup>a</sup>	8.6 (8.2)	6.6 (6.2)
space group	<i>P</i> 6 <sub>5</sub>	<i>P</i> 6 <sub>5</sub>
cell constants	<i>a</i> = <i>b</i> = 92.69 Å <i>c</i> = 47.31 Å α = β = 90°, γ = 120°	<i>a</i> = <i>b</i> = 92.65 Å <i>c</i> = 47.70 Å α = β = 90°, γ = 120°
limiting resolution (Å)	1.90	1.80
completeness of data (%)	100.0 (99.8)	98.2 (100.0)
<i>R</i> <sub>merge</sub> <sup>b</sup> (%)	5.9 (26.9)	7.7 (44.5)
<i>I</i> /σ	45.0 (16.0)	27.5 (3.2)
	Molecular Replacement	
<i>R</i> <sub>cryst</sub> (%)	51.0	
correlation factor <i>C</i> (%)	29.1	
	Refinement	
<i>R</i> <sub>cryst</sub> / <i>R</i> <sub>free</sub> <sup>c</sup> (%)	22.8/26.8	19.8/24.0
no. of non-hydrogen protein atoms	1639	1639
no. of copper atoms	2	2
no. of water molecules	272	215
RMSD <sup>d</sup> (bonds (Å)/angles (deg)/bonded B's (Å <sup>2</sup> ))	0.017/2.83/1.25	0.016/1.75/2.50
mean temp factors (protein/copper/solvent)	21.8/18.2/27.7	24.9/23.2/31.4
dispersion precision indicator (DPI) (Å)	0.21 Å	0.17 Å

<sup>a</sup> Values in parentheses correspond to the highest resolution shell between 1.96 and 1.90 Å [Cu(II) UMC] and 1.85 and 1.80 Å [Cu(I) UMC]. <sup>b</sup> *R*<sub>merge</sub> =  $\sum_h \sum_i |I_i(hkl) - \langle I(hkl) \rangle| / \sum_h \sum_i I_i(hkl)$ . <sup>c</sup> *R*<sub>cryst</sub> =  $\sum_h ||F_o(hkl)| - |F_c(hkl)|| / \sum_h |F_o(hkl)|$ . <sup>d</sup> Root-mean-square deviations of temperature factors of bonded atoms.

the atoms determined by Luzzati plots<sup>33</sup> are 0.27 and 0.18 Å for Cu(II) and Cu(I) UMC, respectively. The more realistic DPIs (dispersion precision indicators) as developed by Cruickshank<sup>34</sup> are lower with values of 0.21 and 0.17 Å obtained for the oxidized and reduced proteins, respectively. The accuracy of the copper ligand bond distances is even higher as reflected by standard deviations of better than 0.06 Å (these were derived from the individual bond distances in the two independent molecules in each structure). The copper site geometry was refined with no stereochemical restraints imposed. The main chain dihedral angles of all non-glycine residues are within energetically allowed regions of the Ramachandran plot [92% and 94.3% in the most favored regions, 8.0% and 5.1% in additionally allowed regions for the Cu(II) and Cu(I) structures, respectively].<sup>35</sup>

**Overall Structure of UMC.** UMC exists as a C<sub>2</sub>-symmetric dimer in the asymmetric unit with intermolecular contacts of 510 Å<sup>2</sup> which corresponds to ca. 9% of the complete surface of the molecule (Figure 1). UMC does not form dimers in solution as the presence of such species was never detected on the gel filtration step used during the purification procedure.<sup>20</sup> The secondary structure of UMC is made up of eight β-strands and two α-helices (see Figures 1 and 2). The strands form two antiparallel β-sheets which give UMC a β-sandwich topology. One of the β-sheets (formed from β-strands 2, 4, 5, 7, and 8) is twisted as in other phycocyanins, and thus, the tertiary structure of UMC lacks the continuity of the Greek key β-barrel topology typically found in cupredoxins.<sup>6,7</sup> The two α-helices of UMC are situated on one side of the β-sandwich, with α-helix 1 being longer in UMC than in CBP, but with a length similar to that found in CST. The second α-helix is shorter than the first and precedes β-strand 5, which is irregular in the phycocyanins and other cupredoxins.<sup>6</sup> The polypeptide linking α-helix 1 and

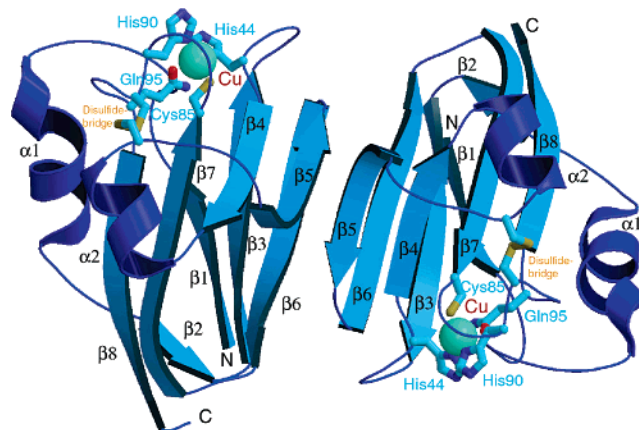


**Figure 1.** Structure of UMC showing the two molecules that make up the dimer arrangement in the asymmetric unit of the oxidized protein. The noncrystallographic 2-fold rotation axis lies perpendicular to the plane of the paper between β-strand 5 of the two molecules. The disulfide bridge is included as are the coordinating side chains, with the copper ion shown as a cyan sphere.

β-strand 5 possesses a Cys residue which forms a disulfide bridge with a Cys found on the copper binding loop (see below). The arrangement of the two UMC molecules in the asymmetric unit involves contacts between residues from the neighboring β-strands 5 and 6 (and also β-strand 3; see Table S1 in the Supporting Information). The copper binding site of UMC is located at one extreme of the molecule (see Figure 1), with the ligands Cys85, His90, and Gln95 found on the active site loop which links β-strands 7 and 8. The coordination of the copper ion is completed by His44, which is located on the loop connecting β-strands 3 and 4. The overall structure of Cu(II) UMC is similar to that of oxidized CST<sup>13</sup> as demonstrated by the fact that the C<sub>α</sub> atoms superimpose with an RMSD of 0.94 Å (see Figure 3). There is also close homology to the structures of CBP<sup>18</sup> and PNC,<sup>19</sup> and these overlap with RMSDs of 1.19 and 1.23 Å, respectively, whereas the similarity to the cupredoxin azurin<sup>11</sup> is lower (RMSD of 1.96 Å).

(33) Luzzati, V. *Acta Crystallogr.* **1952**, *5*, 802–810.

(34) Cruickshank, D. W. J. *Acta Crystallogr.* **1999**, *D55*, 583–601.

(35) Ramchandran, G. N.; Sasisekharan, V. *Adv. Protein Chem.* **1968**, *23*, 283–438.

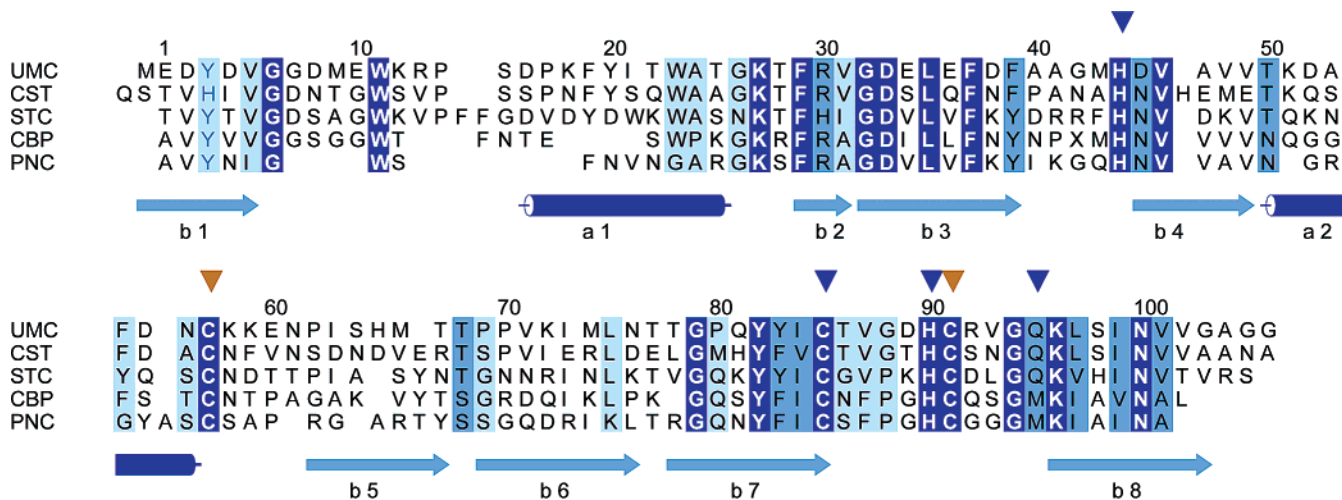


**Figure 2.** Amino acid sequence alignment of UMC,<sup>36</sup> *C. sativus* stellacyanin (CST<sup>37</sup>), the stellacyanin from *Rhus vernicifera* (STC<sup>38</sup>), the plantacyanin from *C. sativus* (CBP<sup>39</sup>), and spinach plantacyanin (PNC<sup>40</sup>). Identical residues in the sequences are highlighted in dark blue. A high level of conservation is indicated in blue, while the regions of relatively low conservation are light blue. The copper binding residues are identified by dark blue arrows, and the two Cys ligands which form the disulfide bridge are indicated with yellow arrows. The secondary structure elements of UMC are indicated as dark blue cylinders ( $\alpha$ -helices) and blue arrows ( $\beta$ -strands).

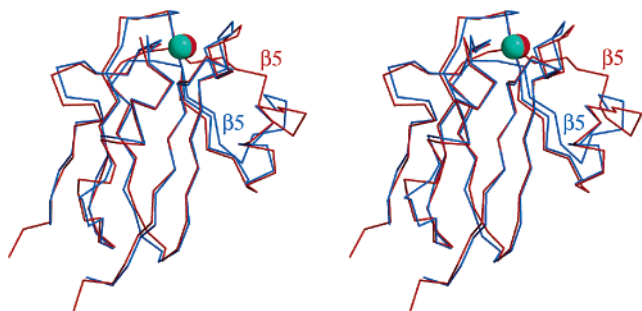


**Figure 3.** A stereoview of an overlay of the C $\alpha$  traces of Cu(II) UMC (blue) and CST<sup>13</sup> (red). The copper atoms are shown as blue and red spheres, respectively, for the two proteins, and the different arrangements of  $\beta$ -strand 5 in UMC and CST can be observed.

UMC possesses a number of Asp and Glu residues close together on its surface which form an acidic patch. This is made up of Glu1, Asp2, Asp4, Asp8, and Glu10 from  $\beta$ -strand 1 and Asp33, Glu34, Glu36, and Asp38 of  $\beta$ -strand 3. These two strands are situated next to each other in the UMC structure, and thus, a large region of negative charge is found on one side of the protein (see Figure 4).

**Active Site.** The coordination geometry of oxidized UMC is distorted tetrahedral with typical Cu(II)–N <sup>$\delta$ 1</sup>(His44) and Cu(II)–N <sup>$\delta$ 1</sup>(His90) distances of 2.0 Å (see Figure 5 and Table 2). The Cu(II)–S $\gamma$ (Cys85) bond length of 2.2 Å is short for a Cu(II)–thiolate but is in the range usually found for type 1 copper sites (see Table 2). The copper ion is displaced from the plane of these three equatorial ligands by  $\sim$ 0.4 Å in the direction of the axial Gln95, which coordinates to Cu(II) via its O $\epsilon^1$  atom at a distance of 2.3 Å. Coordination via the N $\epsilon^2$ H<sub>2</sub> moiety of Gln95 would require deprotonation, which is unlikely given its high pK<sub>a</sub> ( $\sim$ 15). Furthermore, coordination of Gln95 via its O $\epsilon^1$  atom positions the NH<sub>2</sub> group such that a favorable  $\pi$ -amide interaction occurs with the indole ring of Trp11. The backbone carbonyl oxygen of Met43 is found trans to the axial Gln ligand 3.8 Å from the Cu(II) ion.

UMC possesses a number of hydrogen-bonding interactions around its active site which are structurally important. The backbone NH of Cys85 is involved in a hydrogen bond with

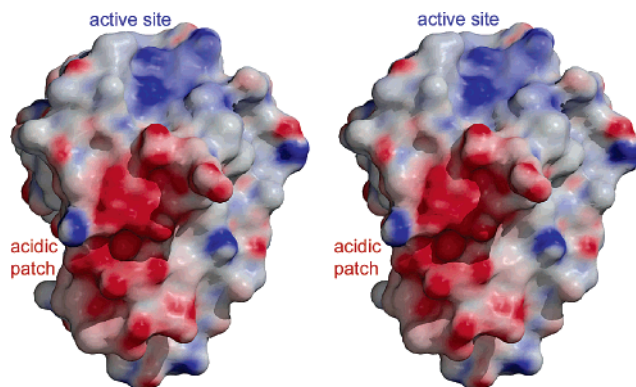


**Figure 4.** A stereoview of the surface properties of UMC showing the acidic patch and the exposed active site His ligands.

the backbone CO of Gln95, which assists in stabilizing the copper-binding loop. There are a number of hydrogen-bonding interactions along the loop (Cys85 to Gln95) including those between the backbone CO groups of Asp89 and His90 and the backbone NH of Val93. The backbone CO of Asp89 also accepts a hydrogen bond from the side chain of Arg92 (the side chain of Asp89 is also involved in a salt bridge with the side chain of Arg13). The residue Asp45, next to the ligand His44, makes a number of key hydrogen-bonding interactions at the active site of UMC. The side chain of Asp45 accepts hydrogen bonds from the backbone NH groups of Thr86 and Val87 and the side chain O $\gamma$ H of Thr86. The backbone CO of Asp45 is hydrogen bonded to the indole N $\epsilon^1$ H of Trp11, while its backbone NH hydrogen bonds to the thiolate sulfur of the Cys85 ligand. The coordinating sulfur of Cys85 also accepts a hydrogen bond from the backbone NH of Val87.

The active site of UMC is solvent exposed, with the imidazole rings of both His ligands protruding through the surface of the protein (the copper is  $\sim$ 4 Å from the surface). The solvent accessibilities of the two His ligands in UMC have been calculated and are shown in Table 3 along with those of other cupredoxins. The degree of solvent exposure is much greater in the phytocyanins than in other cupredoxins. The solvent exposures of the His ligands in UMC are approximately equal,

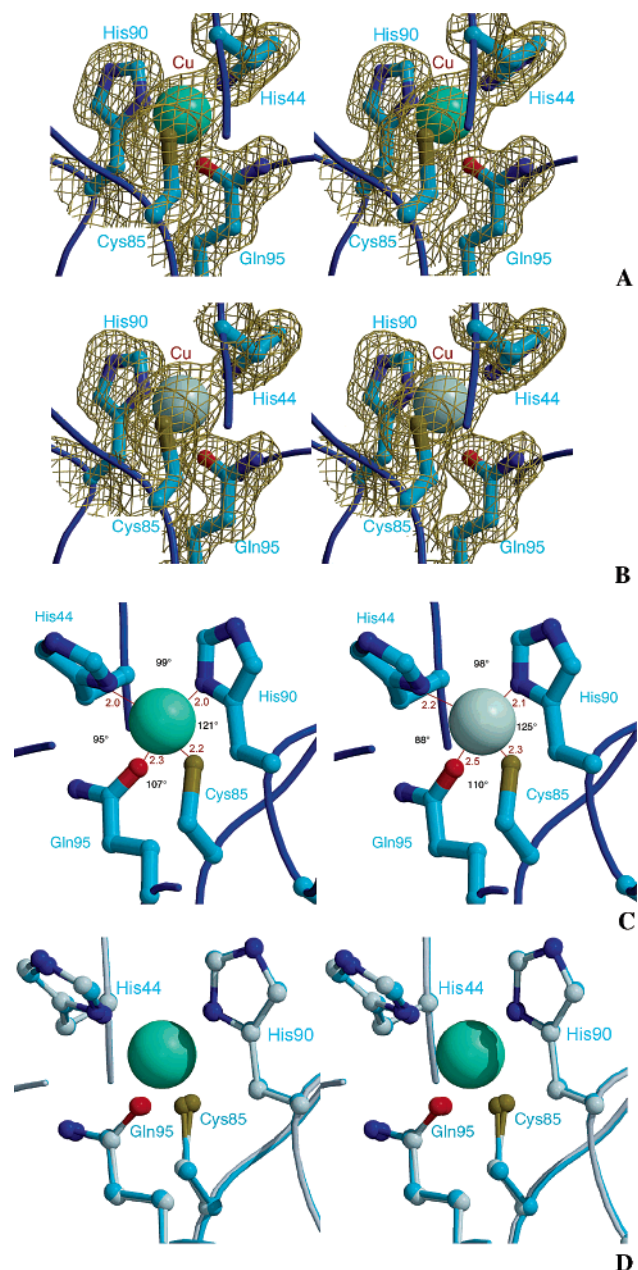


**Figure 5.** (A) A stereoview of the active site of Cu(II) UMC including the  $2F_o - F_c$  electron density map at 1.9 Å resolution contoured at  $1.0\sigma$ . (B) A stereoview of the active site of Cu(I) UMC also showing the  $2F_o - F_c$  electron density map at 1.8 Å resolution contoured at  $1.0\sigma$ . In (C), the active site structures of Cu(II) (left) and Cu(I) (right) UMC are compared and the coordinating residues are shown as ball-and-stick models, with the Cu–ligand distances (Å) and angles (deg) at the active site included. (D) A stereoview of an overlay of the active sites of Cu(II) (cyan backbone and bonds) and Cu(I) (white backbone and bonds) UMC.

whereas in the other cupredoxins the C-terminal His (HisB) is much more exposed. In the structure of UMC, the N<sup>ε2</sup>H of His44 is hydrogen bonded to a water molecule in both the oxidized and reduced structures but there are no water contacts to His90 in either structure.

The exposed imidazole rings of His44 and His90 are surrounded by a protein surface which is made up of both nonpolar and polar residues in UMC. The hydrophobic side chains in this region are provided by Ala40, Met43, Val87, Gly88, and Val93. The polar side chains arise from Glu10, Lys12, Arg13, Ser15, and Asp89 (and His44 and His90). These

residues are randomly arranged, and this region of the protein's surface does not have any uniform properties.

**Structural Changes upon Reduction.** The overall structure of UMC is only slightly altered upon reduction, which is reflected in an RMSD of 0.49 Å for the superimposition of the Cu(II) and Cu(I) structures. Small changes occur in the protein backbone around the C- and N-termini and also in the Gly6 to Met9 and the Ala24 to Lys27 regions. The positions of Pro62, Pro69, and Pro70 are slightly different in the structures of Cu(II) and Cu(I) UMC. These proline residues are situated at the start of  $\beta$ -strands 5 (Pro62) and 6 but are not within 11 Å of the copper ion. The conformations of some side chains on the surface of UMC are altered upon reduction, but the effects are minor.

There are subtle changes at the active site of UMC upon reduction (see Figure 5 and Table 2) which result in a more trigonal pyramidal coordination geometry for the Cu(I) center. An increase in the copper ligand bond distances upon reduction is anticipated due to the larger ionic radius of Cu(I); however, these occur in an anisotropic manner. The Cu(I)–N<sup>δ1</sup>(His90) and Cu(I)–S<sup>γ</sup>(Cys85) bond lengths only increase by  $\sim 0.1$  Å compared to those of the Cu(II) protein, whereas the Cu(I)–N<sup>δ1</sup>(His44) and Cu(I)–O<sup>ε1</sup>(Gln95) bond lengths both increase by  $\sim 0.2$  Å. The changes in the Cu–N<sup>δ1</sup>(His44) and Cu–O<sup>ε1</sup>(Gln95) bond lengths are significantly higher than the largest standard deviation in the bond distances (0.06 Å; see Table 2) and are due to small rotations in the side chains of these two ligands. The displacement of the metal ion from the His<sub>2</sub>Cys plane in Cu(I) UMC ( $\sim 0.3$  Å) is very similar to its position in the oxidized protein. The distance from the Cu(I) ion to the backbone carbonyl oxygen of Met43 (found trans to the axial Gln ligand) is very similar to that in Cu(II) UMC ( $\sim 3.8$  Å).

## Discussion

In this study we have determined the structure of UMC, the cupredoxin domain of the stellacyanin from horseradish roots (the stellacyanins are a subclass of the phytoeyanins) in both the Cu(II) and Cu(I) forms. The structure of the oxidized protein is very similar to that of CST,<sup>13</sup> the only other available stellacyanin structure. This work represents the first determination of the crystal structure of a Cu(I) phytoeyanin (active site information has been published for reduced CST,<sup>41</sup> but a complete structure is not available) and demonstrates the changes that occur in this family of ET proteins upon reduction.

**Overall Structure of UMC.** The dimeric arrangement of two UMC molecules as seen in the asymmetric unit is not prevalent in solution. Analogous arrangements have been observed in a number of cupredoxin crystal structures, and in all cases these are not thought to have any physiological relevance. The sequence homology between UMC and CST is 46% (see Figure 2), and their overall structures are very similar. This is demonstrated in Figure 3, where the C<sup>α</sup> traces of these two molecules are compared. The structure of UMC is also similar to those of the plantacyanins CBP and PNC even though the sequence homology to these proteins is only 30% and 27%, respectively (see Figure 2). These molecules all possess distinctive structural features characteristic of the phytoeyanin subclass of the cupredoxins. The region of largest difference between UMC (and CST) and the plantacyanins involves the region from Trp11 to Trp23 which forms  $\alpha$ -helix 1 in the stellacyanins,

**Table 2.** Geometry of the Active Site of Cu(II) and Cu(I) UMC and Other Cupredoxins

	Cu(II) UMC <sup>a</sup>	Cu(I) UMC <sup>a</sup>	Cu(II) CST <sup>b</sup>	Cu(I) CST <sup>c</sup>	Cu(II) CBP <sup>d</sup>	Cu(II) PNC <sup>e</sup>	Cu(II) PAZ <sup>f</sup>	Cu(I) PAZ <sup>f</sup>	Cu(II) AZ <sup>g</sup>	Cu(I) AZ <sup>g</sup>
Cu–Ligand Bond Distances (Å)										
Cu–N <sup>δ1</sup> (His44)	2.0(0.05)	2.2(0.02)	1.96	2.07	1.93	2.03	1.95	2.04	2.02	2.06
Cu–S <sup>γ</sup> (Cys85)	2.2(0.06)	2.3(0.01)	2.18	2.28	2.16	2.18	2.13	2.19	2.21	2.23
Cu–N <sup>δ1</sup> (His90)	2.0(0.04)	2.1(0.03)	2.04	2.19	1.95	1.99	1.92	2.11	2.08	2.12
Cu–O <sup>ε1</sup> (Gln95)	2.3(0.05)	2.5(0.01)	2.21	2.68						
Cu–S <sup>δ</sup> (Met)					2.61	2.67	2.71	2.85	3.32	3.31
Cu to O(Met43)	3.8	3.8	3.97	na <sup>h</sup>	3.85	4.04	3.94	4.04	2.60	2.67
Angles (deg)										
His44–Cu–Cys85	132	132	134	na	138	137	135	132	132	133
His44–Cu–His90	99	98	101	na	99	100	100	102	105	105
His44–Cu–Gln95(Met)	95	88	94	na	83	81	87	90	72	73
Cys85–Cu–His90	121	125	110	na	110	112	114	116	123	122
Cys85–Cu–Gln95(Met)	107	110	101	na	111	113	107	107	110	110
His90–Cu–Gln95(Met)	95	91	102	na	112	109	107	104	85	87

<sup>a</sup> At pH 5.0. The values quoted are the average of those in the two molecules in the asymmetric unit, and standard deviations are included in parentheses. <sup>b</sup> The stellacyanin from *C. sativus* (at pH 7.0, PDB entry 1JER) in which His46, Cys89, His94, and Gln99 are ligands.<sup>13</sup> The backbone carbonyl oxygen of Ala45 is trans to the axial Gln99 ligand. <sup>c</sup> There is very little information available for the structure of the reduced stellacyanin from *C. sativus*.<sup>41</sup> <sup>d</sup> Cucumber basic protein (at pH 6.0, PDB entry 2CBP) in which His39, Cys79, His84, and Met89 are ligands.<sup>18</sup> The backbone carbonyl oxygen of Met38 is found trans to the axial Met89 ligand. <sup>e</sup> Plantacyanin from spinach (at pH 5.4, PDB entry 1F56) in which His34, Cys74, His79, and Met84 are ligands.<sup>19</sup> The backbone carbonyl oxygen of Gln33 is found trans to the axial Met89 ligand. <sup>f</sup> Pseudoazurin from *Achromobacter cycloclastes* [at pH 6.0; Cu(II), PDB entry 1BQK; Cu(I), PDB entry 1BQR] in which His40, Cys78, His81, and Met86 are ligands.<sup>9</sup> The backbone carbonyl oxygen of Gly39 is found trans to the axial Met86 ligand. <sup>g</sup> Azurin from *Pseudomonas aeruginosa* [at pH 6.5–8.0; Cu(II), PDB entry 1JZF; Cu(I), PDB entry 1JZG] in which His46, Cys112, His117, and Met121 are ligands.<sup>12</sup> The backbone carbonyl oxygen of Gly45 is found trans to Met121. <sup>h</sup> na = information not available.

**Table 3.** Solvent Accessibilities of the His Ligands in the Structures of Cupredoxins

protein	solvent accessibility <sup>a</sup> (Å <sup>2</sup> )		protein	solvent accessibility <sup>a</sup> (Å <sup>2</sup> )	
	HisA	HisB		HisA	HisB
UMC <sup>b</sup>	20.3	24.0	PNC <sup>c</sup>	13.0	29.3
CST <sup>c</sup>	15.4	35.9	azurin <sup>f</sup>	0	4.5
CBP <sup>d</sup>	11.7	26.7			

<sup>a</sup> Calculated using FastSurf<sup>42</sup> and a probe radius of 1.4 Å. <sup>b</sup> HisA = His44, HisB = His90. <sup>c</sup> Stellacyanin from *C. sativus* (PDB entry 1JER), HisA = His46, HisB = His94.<sup>13</sup> <sup>d</sup> Cucumber basic protein (PDB entry 2CBP), HisA = His39, HisB = His84.<sup>18</sup> <sup>e</sup> Plantacyanin from spinach (PDB entry 1F56), HisA = His34, HisB = His79.<sup>19</sup> <sup>f</sup> Azurin from *P. aeruginosa* (PDB entry 4AZU), HisA = His46, HisB = His117.<sup>11</sup>

which is absent in the plantacyanins (see Figures 1 and 2).  $\beta$ -Strand 5 of the cupredoxins is varied in available structures,<sup>6</sup> and in UMC this strand is closer to strand 4 than in the CST structure; thus, the two proteins show larger differences in this region (the RMSD of the C $\alpha$  positions of UMC and CST in this strand is up to 3 Å, whereas in the other parts of the molecule it is less than 1.0 Å; see Figure 3). The polypeptide linking  $\alpha$ -helix 2 and  $\beta$ -strand 5 contains a Cys residue that forms a disulfide bridge with a Cys on the ligand-containing loop, which stabilizes this region of the structure. In the dimer arrangement in the asymmetric unit of UMC  $\beta$ -strand 5 is found at the interface between the two molecules, and the compact arrangement of this part of the structure of UMC enables a strong dimer interface. The structure of  $\beta$ -strand 5 is very similar in both Cu(II) and Cu(I) UMC, and therefore, the fact that this area is variable does not mean that it is flexible.

Native UMC is glycosylated at Asn76, with the amount of carbohydrate varying between 2% and 9%.<sup>36</sup> The recombinant protein studied herein lacks the surface sugar but has spectroscopic properties identical to those of the native protein.<sup>20</sup> The residue Asn76 is located at the bottom of  $\beta$ -strand 6 close to the C-terminus of the protein. Native UMC possesses a C-terminal domain which is closely related to those found in a

class of plant cell wall proteins, the arabinogalactans.<sup>36</sup> The presence of carbohydrate close to the link between the cupredoxin and C-terminal arabinogalactan-like domain suggests a role in either protecting this region from proteolytic enzymes or in maintaining a specific spatial arrangement of the two domains. In the CST structure Asn109, the site of glycosylation, is also situated very close to the interdomain region.<sup>13</sup> This stellacyanin also possesses about 10% carbohydrate, which probably has a function similar to that in UMC.

The prominent surface feature of UMC is a large acidic patch on one side of the molecule (see Figure 4). CST possesses a similarly sized acidic patch (eight residues), but this is made up of residues from  $\beta$ -strands 4–6. Thus, the acidic patch of UMC is found on the side of the  $\beta$ -sandwich, whereas in CST it is located on the front. Comparison of available phytoeyanin sequences<sup>1–3</sup> indicates that the only other member which possesses an acidic patch in the same position as UMC is BCB, a stellacyanin from *A. thaliana*. The cupredoxin domain of this stellacyanin has ~81% identity to that of UMC, and a recent study has demonstrated the similarity between the active sites of the two proteins.<sup>20</sup> No other phytoeyanin possesses an acidic patch in a position similar to that found in CST.<sup>1–3</sup> The two structurally characterized plantacyanins CBP and PNC are basic proteins and have large positively charged surface patches. These are found in positions completely different from those of the acidic surfaces on UMC and CST and are located at the opposite end of the  $\beta$ -sandwich to the copper site. It has been suggested that the exposed nature of the active sites of the phytoeyanins indicates interaction with small molecule redox partners.<sup>1,2,18</sup> However, the presence of surface-charged regions on the phytoeyanins would suggest a role in protein–protein ET as a number of cupredoxins possess charged surface patches which are key to their interaction with physiological redox part-

(37) Mann, K.; Schäfer, W.; Thoenes, U.; Messerschmidt, A.; Mehrabian, Z.; Nalbandyan, R. *FEBS Lett.* **1992**, *314*, 220–223.

(38) Bergman, C.; Gandvik, E.-A.; Nyman, P. O.; Strid, L. *Biochem. Biophys. Res. Commun.* **1997**, *77*, 1052–1059.

(39) Murata, M.; Begg, G. S.; Lambrou, F.; Leslie, B.; Simpson, R. J.; Freeman, H. C.; Morgan, F. J. *Proc. Natl. Acad. Sci. U.S.A.* **1982**, *79*, 6434–6437.

(36) Van Driessche, G.; Dennison, C.; Sykes, A. G.; Van Beeumen, J. *Protein Sci.* **1995**, *4*, 209–227.

ners.<sup>16,43–47</sup> The fact that the stellacyanins possess cell wall anchoring domains does not preclude a role in interprotein ET. The site of glycosylation in UMC (Asn76) is situated some distance from the majority of the acidic patch, and thus, the relatively small amount of sugar is unlikely to mask this surface feature.

Almost all cupredoxins possess a hydrophobic patch surrounding the exposed imidazole ring of the C-terminal His ligand.<sup>6,7</sup> This region is important for the interaction with ET partners,<sup>15–17</sup> and it is thought to be exclusively used as the route of entry and exit of electrons to and from the copper site. In the structure of UMC, as in those of all other phytocyanins,<sup>13,18,19</sup> both His ligands are solvent exposed (vide infra), but the protein surface in this area is not exclusively hydrophobic (see Figure 4). The region not only contains polar residues but also possesses charged side chains. The lack of a clear hydrophobic patch around the exposed His ligands is a feature shared by CST and thus may be common to the stellacyanins. In CBP and PNC (plantacyanins) there are also hydrophobic and hydrophilic side chains in this area, although there are no charged residues. Furthermore, there is a clear hydrophobic patch around the exposed imidazole ring of the C-terminal His ligand in the two plantacyanin structures. This supports the idea that the lack of a hydrophobic patch is a feature common to the stellacyanins (and not all phytocyanins) and must be related to the partners with which these molecules interact. The variable features of the surface patches of the phytocyanins suggest that relatively relaxed evolutionary constraints have been imposed on the protein scaffold, which has allowed a range of attributes to evolve for binding to specific partners.

**Active Site.** The distorted tetrahedral geometry of the Cu(II) site of UMC, with Gln95 coordinating in a monodentate fashion via its O<sup>ε1</sup> atom and providing a fourth strong ligand (see Figure 5), is remarkably similar to that of oxidized CST (see Table 2). This arrangement is also analogous to that found at the active site of the Cu(II) Met121Gln azurin mutant,<sup>48</sup> which was made as a model for the active site of the stellacyanins. The interaction of the cupric ion with the three equatorial ligands in all of these proteins is similar to that seen in cupredoxins with a weak axial Met ligand.<sup>6–12,18,19</sup> A possible exception to this is the Cu(II)–S<sup>γ</sup>(Cys) bond, which appears slightly longer in the stellacyanins. This is consistent with the results of various spectroscopic investigations<sup>5,14,49–53</sup> and has been attributed to the strong

interaction of the cupric ion with the Gln ligand in the stellacyanins, which results in a weakening of the Cu(II)–S<sup>γ</sup>(Cys) bond. However, given the resolution of the available crystal structures, we cannot be sure that these differences are really significant.

The close similarity of the active site structures of Cu(II) UMC and CST is surprising when their spectroscopic features are compared. The UV/vis spectrum of Cu(II) UMC is dominated by an intense S(Cys) → Cu(II) LMCT band at 606 nm with a second weak LMCT transition (also involving the Cys ligand) at 463 nm.<sup>5,20,54</sup> The low intensity of the 463 nm band, along with the axial EPR spectrum for the protein, results in UMC having a classic type 1 copper site.<sup>5,20,53</sup> In most other stellacyanins (including CST) the LMCT band at ~450 nm is more intense, and they have rhombic EPR spectra, which indicates the presence of perturbed type 1 copper centers.<sup>5,20,53</sup> It has been suggested<sup>51</sup> that the displacement of the copper ion from the His<sub>2</sub>Cys ligand plane, as a consequence of a stronger axial interaction, results in a site with perturbed spectroscopic properties. However, the distances of the Cu(II) ion from this plane are similar in both UMC and CST (~0.4 and 0.3 Å, respectively). More recently, the electronic properties of type 1 copper sites with an axial Met ligand have been rationalized by the coupled distortion model<sup>52</sup> in which a more perturbed center is associated with an enhanced Cu–S<sup>δ</sup>(Met) interaction, which leads to a weaker Cu–S<sup>γ</sup>(Cys) bond and collectively results in a Jahn–Teller distortion. This alteration is quantified by the angle between the N<sub>His</sub>CuN<sub>His</sub> and S<sub>Cys</sub>CuS<sub>Met</sub> planes, with a smaller value consistent with a perturbed site. The angles between the N<sub>His</sub>CuN<sub>His</sub> and S<sub>Cys</sub>CuO<sub>Gln</sub> planes are 89° and 84° in Cu(II) UMC and CST, respectively. This difference, along with the slightly longer Cu(II)–O<sup>ε1</sup>(Gln95) bond in UMC (see Table 2), could account for the electronic variations compared to CST.

A unique feature of the active site of the stellacyanins is the interaction of the axial ligand with the indole ring of a Trp residue. Coordination of the Gln via its O<sup>ε1</sup> atom results in a N<sup>ε2</sup>H moiety pointing toward the center of the five-membered ring of the Trp. This provides a favorable interaction between the π-electron density of the indole and the partial positive charge on the amide proton. In the plantacyanins the methyl group of the axial Met ligand points to the center of the side chain of the corresponding Trp residue.<sup>18,19</sup> A conserved feature of cupredoxins is that the axial ligand is sandwiched between two hydrophobic residues,<sup>6</sup> but the interaction appears to be stronger in the phytocyanins (the Gln/Met to Trp separation in the phytocyanins is ~3.5 Å, whereas in other cupredoxins the distance to the corresponding, usually aromatic, residue is ~4.5 Å). The importance of the interaction of the axial ligand with the indole ring in the phytocyanins is currently under investigation by site-directed mutagenesis.

The intricate hydrogen-bonding pattern at the active site of UMC is similar to that found in other phytocyanins (and

- (40) Mann, K.; Eckerskorn, C.; Mehrabian, Z.; Nalbandyan, R. M. *Biochem. Mol. Biol. Int.* **1996**, *40*, 881–887.
- (41) Nersissian, A. M.; Hart, J. P.; Valentine, J. S. In *Handbook of Metalloproteins*; Messerschmidt, A., Huber, R., Poulos, T., Wieghardt, K., Eds.; John Wiley and Sons: Chichester, U.K., 2001; pp 1219–1234.
- (42) Tsodikov, O. V.; Record, M. T.; Sergeev, Y. V. *J. Comput. Chem.* **2002**, *23*, 600–609.
- (43) Kannt, A.; Young, S.; Bendall, D. S. *Biochim. Biophys. Acta* **1996**, *1277*, 115–126.
- (44) Sato, K.; Kohzuma, T.; Dennison, C. *J. Am. Chem. Soc.* **2004**, *126*, 3028–3029.
- (45) Kukimoto, M.; Nishiyama, M.; Ohnuki, T.; Turley, S.; Adman, E. T.; Horinouchi, S.; Beppu, T. *Protein Eng.* **1995**, *8*, 153–158.
- (46) Williams, P. A.; Fülöp, V.; Leung, Y. C.; Chan, C.; Moir, J. W. B.; Howlett, G.; Ferguson, S. J.; Radford, S. E.; Hajdu, J. *Nat. Struct. Biol.* **1999**, *2*, 975–982.
- (47) De Rienzo, F.; Gabdoulline, R. R.; Menziani, M. C.; Wade, R. C. *Protein Sci.* **2000**, *9*, 1439–1454.
- (48) Romero, A.; Hoitink, C. W. G.; Nar, H.; Huber, R.; Messerschmidt, A.; Canters, G. W. *J. Mol. Biol.* **1993**, *229*, 1007–1021.
- (49) DeBeer, S.; Randall, D. W.; Nersissian, A. M.; Valentine, J. S.; Hedman, B.; Hodgson, K. O.; Solomon, E. I. *J. Phys. Chem. B* **2000**, *104*, 10814–10819.
- (50) Bertini, I.; Fernández, C. O.; Karlsson, B. G.; Leckner, J.; Luchinat, C.; Malmström, B. G.; Nersissian, A. M.; Pierattelli, R.; Shipp, E.; Valentine, J. S.; Vila, A. J. *J. Am. Chem. Soc.* **2000**, *122*, 3701–3707.

- (51) Andrew, C. R.; Yeom, H.; Valentine, J. S.; Karlsson, B. G.; Bonander, N.; van Pouderoyen, G.; Canters, G. W.; Loehr, T. M.; Sanders-Loehr, J. *J. Am. Chem. Soc.* **1994**, *116*, 11489–11498.
- (52) LaCroix, L. B.; Randall, D. W.; Nersissian, A. M.; Hoitink, C. W. G.; Canters, G. W.; Valentine, J. S.; Solomon, E. I. *J. Am. Chem. Soc.* **1998**, *120*, 9621–9631.
- (53) Solomon, E. I.; Szilagyi, R. K.; De Beer George, S.; Basumallick, L. *Chem. Rev.* **2004**, *104*, 419–458.
- (54) Dennison, C.; Lawler, A. T. *Biochemistry* **2001**, *40*, 3158–3166.

cupredoxins) and is key to stabilizing the active site structure. The residue Asp45, next to the His44 ligand, is involved in a number of these interactions. This residue is an Asn in almost all other phytoacyanins and cupredoxins (see Figure 2 and ref 1). The presence of an Asp in UMC has very little influence on the number of hydrogen-bonding interactions. The thiolate sulfur of Cys85 accepts hydrogen bonds from the backbone NH groups of Asp45 and Val87. The second hydrogen bond is not found in cupredoxins which have a Pro two residues after the Cys ligand (plastocyanin, amicyanin, and pseudoazurin, for example). Azurin and probably all phytoacyanins have this hydrogen bond, which has been suggested to possibly be important for controlling the reduction potential and spectroscopic properties of a type 1 copper site<sup>6</sup> and also the  $pK_a$  of the C-terminal His ligand (vide infra) in reduced cupredoxins.<sup>18</sup>

In UMC, as in all phytoacyanin structures, the copper ion is closer to the surface ( $\sim 4$  Å) than usually found in cupredoxins ( $\sim 5$ – $7$  Å). This leads to increased solvent accessibility of the active site, and the imidazole rings of both His ligands protrude through the surface of the protein (see Table 3). In UMC His90 is slightly more solvent exposed than His44, but the difference is not as large as in the other phytoacyanins. The overall solvent accessibility of the active site of UMC seems to be slightly higher than in the plantacyanins, but is less than that found in CST, which is consistent with the results of NMR studies.<sup>5,54</sup> The reduction potential of UMC is 290 mV,<sup>54</sup> whereas those of CST, CBP, and PNC are 260 mV,<sup>2</sup> 304 mV,<sup>55</sup> and 345 mV,<sup>56</sup> respectively. The stellacyanin from *R. vernicifera* (STC), whose structure has not been determined, has the lowest reduction potential known (185 mV) for a type 1 copper site.<sup>3</sup> There does not appear to be any direct relationship between the solvent exposure of the active sites of the phytoacyanins and their reduction potentials. This is consistent with the results of recently published quantum mechanical calculations which indicate that desolvation of type 1 copper sites is not a significant determinant of their relative reduction potentials.<sup>57</sup>

The changes in the structure of the active site of UMC upon reduction (see Table 2) can partly be rationalized by the increased size of the Cu(I) ion. The largest change involves the axial Gln95 ligand, which twists away from the metal ion upon reduction, resulting in a  $\sim 0.2$  Å increase in the Cu to O<sup>e1</sup> distance. We consider the resulting Cu(I) to O<sup>e1</sup>(Gln95) separation of 2.5 Å to represent a bond,<sup>58,59</sup> albeit a relatively weak one. This change and the lengthening of the Cu–N<sup>o1</sup>(His44) bond by  $\sim 0.2$  Å upon reduction cause a subtle alteration in geometry from distorted tetrahedral to more trigonal pyramidal in Cu(I) UMC. The full structure of Cu(I) CST has not been published, but some active site information has been reported<sup>41</sup> including an increase in the Cu–O<sup>e1</sup>(Gln) distance of  $\sim 0.5$  Å upon reduction (see Table 2) and the suggestion that there is a break in electron density between the copper and the oxygen. The Met121Gln azurin variant undergoes even greater active site alterations upon reduction, resulting in the Cu(I) ion being 2-coordinate,<sup>48</sup> and therefore does not provide an accurate

picture of the redox-induced active site changes in stellacyanins. It appears from the reported structural details that the Cu–S<sup>γ</sup>–(Cys) bond also increases more upon reduction in CST than in UMC. However, recent EXAFS studies on CST have reported a much smaller change in the copper–thiolate bond length upon reduction.<sup>60</sup> In UMC the limited alterations at the active site upon reduction are not too dissimilar from those observed at the copper centers of cupredoxins with axial Met ligands (see Table 2). Thus, the active site of UMC is an example of an entatic state where the rigid protein holds the copper center in a geometry which undergoes only small changes upon redox interconversion, and thus, the inner sphere reorganization energy is minimized.<sup>61</sup> It is interesting to note that the electron self-exchange (ESE) rate constant of UMC is relatively small for a cupredoxin, and that the Gln95Met UMC variant has enhanced (5-fold) ESE reactivity, demonstrating that an axial Met ligand is actually preferable for fast ET.<sup>62</sup>

The rigid copper site environment of UMC is interesting when considering the alkaline transition in phytoacyanins. This effect leads to a change in color of the Cu(II) protein from blue at neutral pH to violet at pH > 9–10.<sup>3,54,63</sup> A number of suggestions have been made for the structural cause of the alkaline transition, with flexibility of the active site being proposed as a major contributing factor.<sup>41,63</sup> The structures of Cu(II) and Cu(I) UMC show that the active site of this protein is rigid, strongly suggesting that flexibility is not responsible for the alkaline transition. Attempts to obtain structural information on the alkaline form of Cu(II) UMC were unsuccessful due to the instability of the crystals under these conditions.

The crystallographic studies on UMC were carried out at pH 5.0, and in the reduced structure there is no evidence that either of the His ligands is becoming protonated and is dissociating from the metal ion [the Cu–N<sup>o1</sup>(His44) bond does lengthen slightly upon reduction]. Protonation and dissociation of the C-terminal His ligand has been observed in a number of reduced cupredoxins<sup>64,65</sup> including some phytoacyanins.<sup>55,56</sup> This effect is important as it has a dramatic influence on the reduction potential<sup>66</sup> and also the ET reactivity<sup>67,68</sup> of a type 1 copper site. Herein, we demonstrate that there is very little change in the Cu–N<sup>o1</sup>(His90) bond length upon reduction, which is supported by NMR studies which show that both His ligands are not protonated at pH 3.5 in Cu(I) UMC.<sup>69</sup> The additional hydrogen bond to the thiolate sulfur of the Cys85 ligand from the backbone NH of Val87 may help to stabilize the active site loop in UMC, thus lowering the  $pK_a$  for the His ligand in the Cu(I) protein.<sup>18</sup> However, this hydrogen bond is present in

(55) Battistuzzi, G.; Borsari, M.; Loschi, L.; Sola, M. *J. Biol. Inorg. Chem.* **1997**, *2*, 350–359.

(56) Battistuzzi, G.; Borsari, M.; Loschi, L.; Sola, M. *J. Inorg. Biochem.* **1998**, *69*, 97–100.

(57) Li, H.; Webb, S. P.; Ivancic, J.; Jensen, J. H. *J. Am. Chem. Soc.* **2004**, *126*, 8010–8016.

(58) Hendricks, H. M. J.; Birker, P. J. M. W. L.; van Rijn, J.; Verschoor, G. C.; Reedijk, J. *J. Am. Chem. Soc.* **1982**, *104*, 3607–3617.

(59) Sorell, T. N.; Malachowski, M. R. *Inorg. Chem.* **1983**, *22*, 1883–1887.

(60) DeBeer George, S.; Basumallick, L.; Szilagyi, R. K.; Randall, D. W.; Hill, M. G.; Nersissian, A. M.; Valentine, J. S.; Hedman, B.; Hodgson, K. O.; Solomon, E. I. *J. Am. Chem. Soc.* **2003**, *125*, 11314–11328.

(61) Gray, H. B.; Malmström, B. G.; Williams, R. J. P. *J. Biol. Inorg. Chem.* **2001**, *5*, 551–559.

(62) Harrison, M. D.; Dennison, C. *ChemBioChem* **2004**, *5*, 1579–1581.

(63) Fernández, C. O.; Sannazzaro, A. I.; Vila, A. J. *Biochemistry* **1997**, *36*, 10566–10570.

(64) Guss, J. M.; Harrowell, P. R.; Murata, M.; Norris, V. A.; Freeman, H. C. *J. Mol. Biol.* **1986**, *192*, 361–387.

(65) Dennison, C.; Lawler, A. T.; Kohzuma, T. *Biochemistry* **2002**, *41*, 552–560.

(66) Armstrong, F. A.; Hill, H. A. O.; Oliver, B. N.; Whitford, D. J. *Am. Chem. Soc.* **1985**, *107*, 1473–1476.

(67) Sato, K.; Kohzuma, T.; Dennison, C. *J. Am. Chem. Soc.* **2003**, *125*, 2101–2112.

(68) Di Bilio, A. J.; Dennison, C.; Gray, H. B.; Ramirez, B. E.; Sykes, A. G.; Winkler, J. R. *J. Am. Chem. Soc.* **1998**, *120*, 7551–7556.

(69) Sato, K.; Dennison, C. Unpublished results.

phytyocyanins in which this effect has been demonstrated,<sup>55,56</sup> and the structural causes of His ligand protonation remain elusive.<sup>65</sup>

### Conclusions

The overall structure of Cu(II) UMC is very similar to those of oxidized CST, CBP, and PNC. Subtle variations at the active sites of Cu(II) UMC and CST account for the former possessing a classic type 1 site and CST having a distorted center. The structure of Cu(I) UMC is very similar to that of the oxidized protein including at the active site where the largest changes involve  $\sim 0.2$  Å increases in the Cu–N<sup>δ1</sup>(His44) and Cu–O<sup>ε1</sup>-(Gln95) bond lengths. The observation that this phytyocyanin possesses an entatic active site, and a charged surface patch,

confirms that these ubiquitous plant proteins function in protein–protein electron transfer.

**Acknowledgment.** This work was supported by BBSRC (Grant No. 13/B16498). We thank Ben Allen and Prof. A. Harriman for assistance with molecular visualization software. We are indebted to Prof. Robert Huber for continuous support and interest in this work.

**Supporting Information Available:** A table showing the nearest approaches between the two molecules in the dimer arrangement in the asymmetric unit of Cu(II) UMC (PDF). This material is available free of charge via the Internet at <http://pubs.acs.org>.

JA046184P